Bioorganic & Medicinal Chemistry Letters 21 (2011) 6094–6099

Contents lists available at SciVerse ScienceDirect

Bioorganic & Medicinal Chemistry Letters

journal homepage: www.elsevier.com/locate/bmcl

Synthesis and structure–activity relationships of novel substituted 8-amino, 8-thio, and 1,8-pyrazole congeners of antitubercular rifamycin S and rifampin

Yafei Jin [a], Sumandeep K. Gill [b], Paul D. Kirchhoff [a], Baojie Wan [d], Scott G. Franzblau [d], George A. Garcia [b,c], H.D. Hollis Showalter [a,c,*]

[a] Vahlteich Medicinal Chemistry Core, University of Michigan, Ann Arbor, MI 48109-1065, USA
[b] Interdepartmental Program in Chemical Biology, University of Michigan, Ann Arbor, MI 48109-1065, USA
[c] Department of Medicinal Chemistry, University of Michigan, Ann Arbor, MI 48109-1065, USA
[d] Institute for Tuberculosis Research, College of Pharmacy, University of Illinois, Chicago, IL 60612-723, USA

ARTICLE INFO

Article history:
Received 27 May 2011
Revised 9 August 2011
Accepted 11 August 2011
Available online 19 August 2011

Keywords:
Rifamycin
MTB
Escherichia coli
MIC_{90}
RNAP

ABSTRACT

A series of rifamycin S and rifampin analogues incorporating substituted 8-amino, 8-thio, and 1,8-pyrazole substituents has been synthesized. The compounds were made by activation of the C-8 phenol as a sulfonate ester, followed by displacement with selected nitrogen and sulfur nucleophiles. The analogues were screened in assays to quantify their antitubercular activity under both aerobic and anaerobic conditions, and for inhibition of wild-type *Mycobacterium tuberculosis* (MTB) RNAP and rifamycin-resistant MTB RNAP (S450L) via an in vitro rolling circle transcription assay. Additionally, the MIC_{90} values were determined for these analogues against *Escherichia coli* strains. Although none of the analogues displayed superior enzymatic or microbiological activity to their parent scaffolds, the results are consistent with the Rif C-8 hydroxyl acting as a hydrogen bond acceptor with S450 and that Rif resistance in the S450L mutant is due to loss of this hydrogen bond. Representative analogues were also evaluated in the human pregnane X receptor (PXR) activation assay.

With nearly one-third of the global population infected by *Mycobacterium tuberculosis* (MTB), tuberculosis (TB) is still a major cause of death. Indeed, in 2006 over nine million new cases and 1.7 million deaths occurred due to TB, and there is now significant concern about the emergence of multi-drug resistant (MDR) strains of TB with an estimated 0.5 million cases worldwide.[1] Despite these appalling statistics, there have been relatively few new agents discovered in the past 40 years to treat this disease.

The rifamycins are members of the ansamycin family of antibiotics, consisting of an ansa, poly-hydroxylated bridge connecting two ends of a naphthoquinone (or naphthohydroquinone) core. They display activity against mycobacteria as well as Gram-positive bacteria and, to a lesser extent, Gram-negative bacteria. Particularly attractive with the rifamycins is their sterilizing activity. This effect also applies to slowly metabolizing extra-cellular bacilli (persisters), a feature possessed by few other TB drugs.[2,3] Mechanistically, the rifamycins exhibit specific inhibition of DNA-dependent RNA synthesis[3–9] with binding constants for prokaryotic RNA polymerases in the range of 10^{-8} M whereas those for eukaryotic enzymes are at least 10,000 times weaker. Amongst the clinically utilized rifamycins, rifampin (RMP, **1**) is the most widely utilized worldwide. This agent totally blocks the translocation step that normally follows formation of the first phosphodiester bond by the polymerase, suggesting that rifamycins sterically block the extension of the RNA chain at a very early stage.[10] The binding site for the rifamycins on RNA polymerase (RNAP) has been shown to be at the β subunit encoded by the *rpoB* gene. A key breakthrough has been the determination of the X-ray crystal structures of several different rifamycins bound to RNAP.[11] These studies show the polymerase to form key hydrogen bond interactions with the four hydroxyl groups (at C-1, C-8, C-21, and C-23) of rifampin, consistent with the known structure–activity relationships (SAR) of the rifamycins, as well as the carbonyl oxygen of the C-25 acetoxy group, and help explain the high resistance that results from single point mutations of amino acids found to have direct interactions with the naphthalene backbone.

We have recently published a comprehensive review on the rifamycins, which includes an extensive analysis of prior SAR reports.[12] While initial SAR studies indicated that most modifications of the ansa bridge led to less active compounds, those on the naphthalene ring were much better tolerated, with the significant exception that acetylation of the C-8 hydroxyl group eliminated activity.[13] A wide variety of substitutions at C-3 were found to be well tolerated, which has been exploited toward the development of several clinical agents.[13–15]

Due to the general paucity of C-8 functionalized rifamycin analogues, we decided to explore the SAR of this position in greater

* Corresponding author.
E-mail address: showalh@umich.edu (H.D.H. Showalter).

0960-894X/$ - see front matter © 2011 Elsevier Ltd. All rights reserved.
doi:10.1016/j.bmcl.2011.08.054

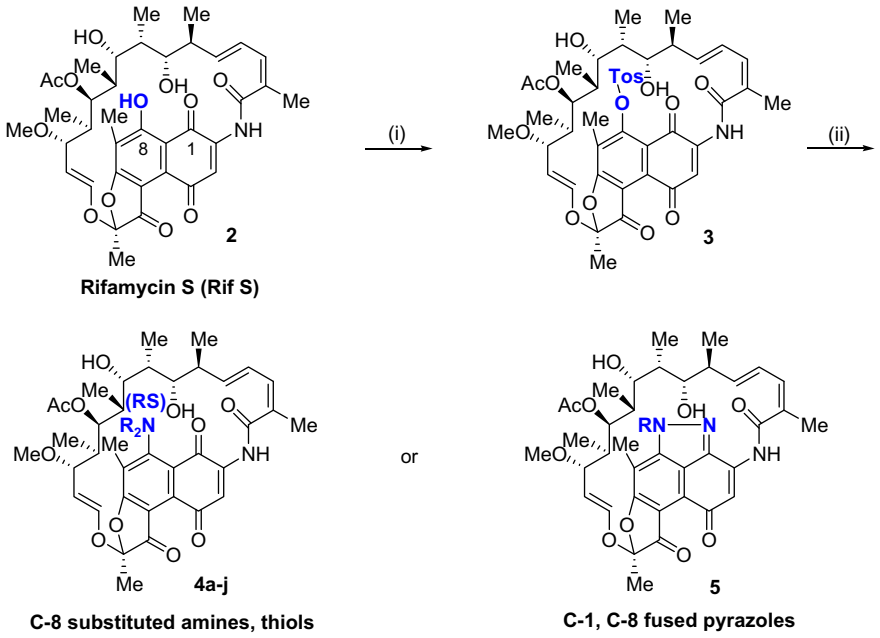

Scheme 1. Synthesis of C-8 analogues of rifamycin S. (i) *p*-toluenesulfonyl chloride, diisopropylethylamine, acetonitrile; (ii) R_2NH, or $RNHNH_2$, or RSNa in acetonitrile (5–80% yield).

depth by applying an 'enabling reaction' that we had reported on several years ago.[16] This involved the facile activation of the 1-hydroxy function of 9,10-anthracendiones toward displacement by nitrogen and sulfur nucleophiles, which we believed could also be applied to the napthoquinone core of rifamycin S (Rif S, **2**) and related congeners.

Our strategy was to first activate the C-8 peri-phenolic functionality of readily available Rif S (**2**) as a sulfonate ester, and then displace this with selected nitrogen nucleophiles through an addition–elimination mechanism (Scheme 1). Given that the rifamycin framework is embellished with so much functionality, including free hydroxyl groups at C-21 and C-23 (Fig. 1), we first needed to work out conditions for selective functionalization of the C-8 phenolic moiety. Thus, the reaction of Rif S (**2**) with sulfonyl chlorides representing a range of reactivity (*p*-toluenesulfonyl, *p*-chlorosulfonyl, methanesulfonyl) and triflic anhydride was evaluated under different temperature and solvent conditions. Of these, only *p*-toluenesulfonyl and *p*-chlorosulfonyl sulfonate esters formed cleanly under optimum conditions (Hunig's base, acetonitrile, room temperature) with tosylate **3** formed in 84% yield. Subsequent reactions of these with amines and hydrazines indicated that the *p*-chlorosulfonate ester was susceptible to cleavage to Rif S, whereas the *p*-toluenesulfonate ester provided the desired C–O bond displacement. With this finding, condensation of **3** was then carried out with a range of amines to provide adducts **4a**–**4i** in 11–51% yields, and with (2-hydroxyethyl)hydrazine to give annulated pyrazole product **5** in very low (5%) yield. We also tested tosylate displacement with a single thiol (methanethiol sodium salt), which provided analogue **4j** in poor yield. Having developed the chemistry for Rif S, we then applied it toward making related analogues of RMP (**1**, Scheme 2). Thus, oxidation of RMP with potassium ferricyanide provided rifampin S (RMP S, **6**) in 65% yield. Tosylation of the 8-hydroxyl function was conducted as described above to give key intermediate **7** in nearly quantitative yield. Amination of **7** was then carried out with several of the same amines utilized above to give adducts **8a**–**8f** in 35–60% yields and pyrazoles **9a** (33% yield) and **9b** (40% yield). Disappointingly, an attempt to make the simple unsubstituted pyrazole congener derived from hydrazine was unsuccessful. Similarly, we were unable to secure a highly sought for analogue derived from ammonia displacement of tosylate **7**. Utilizing the same conditions that gave **4a** led to a product in 46% yield that both mass spec and NMR data showed incorporation of the NH_2 function, but without loss of the C-8 tosyloxy moiety. The NMR spectrum was too complex to make a definitive structural assignment. Candidate possibilities include Michael addition of ammonia to the dienone function or to the imino double bond of the side chain hydrazone. MIC testing of this compound versus two MTB strains (*vide infra*) showed it to be completely inactive. The quinone function of each RMP S amine adduct was then reduced with ascorbic acid to the hydroquinone form, providing corresponding RMP C-8 amine congeners **10a**–**10f** in 51–93% yield. The full range of synthesized compounds is shown in Table 1.

No effort was made to optimize the reaction conditions that provided amine, thiol, or pyrazole adducts from tosylates **3** or **7**, and product yields in general represent a single run for each target compound. All compounds were rigorously purified by preparative silica gel chromatography, and their structural assignments were supported by diagnostic peaks in the ^1H NMR spectra and by mass spectrometry.

Apart from a previous report of the synthesis of Rif S ammonia adduct **4a** in the patent literature,[17] no other analogues have ever been reported in which C-8 substituents derived from amine or sulfur nucleophiles have been incorporated onto a rifamycin scaffold. Furthermore, despite many elaborations of the parent rifamycin scaffold onto the 'southeastern' part of the naphthoquinone template, including ring annulations (e.g., rifalazil[18]), we are unaware of any ring fusions onto the 1,8-carbon positions. Hence our synthesis of pyrazoles **5**, **9a**, and **9b** represents the first report of such a core modification.

Results and discussion

The compounds were screened in assays to quantify their antitubercular activity under both aerobic and anaerobic conditions (Table 1). Briefly, the 8 day microplate-based assay using Alamar blue reagent (added on day 7) for determination of growth (MABA)[19] gives an assessment of activity against replicating MTB,

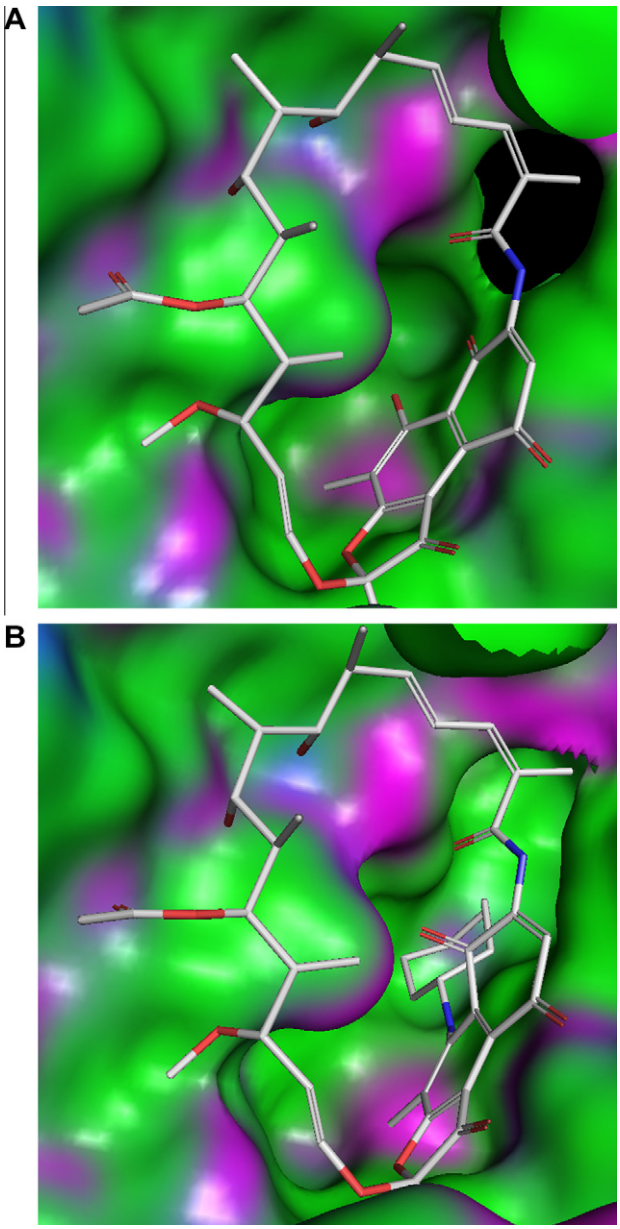

Figure 1. RNAP is shown as a molecular surface within 5 Å of the inhibitors (carbon atoms shown in gray) and shaded to indicate areas of lipophilicity (green), hydrogen bonding (magenta) and mild polar (blue). (A) Rif S (**2**). (B) Cycloheptylamino analogue (**4i**).

while the 11 day high-throughput, luminescence-based low-oxygen-recovery assay (LORA)[20] measures activity against bacteria in a non-replicating state that models clinical persistence. Minimum inhibitory concentrations (MIC_{90}s) are defined as the lowest compound concentration effecting >90% growth inhibition.

Under aerobic conditions (MABA) within the Rif S series, analogues incorporating C-8 amine substituents display modest MIC_{90}s (1.4–5.6 μM) relative to the parent Rif S **2** (0.03 μM). The unsubstituted NH_2 analogue is best (compare **4a** vs **4b**–**4i**), although within this small series there is no significant variation from the smallest to the largest substituent. In addition the installation of small polar functionality (e.g., **4e**, **4g**) or bulky lipophilic moieties (e.g., **4h**, **4i**) seems to impart minimal effect on potency. Activity under anaerobic conditions (LORA) mirrors much the same pattern with only **4c** displaying modest activity (5.4 μM), and with compound MIC_{90}s ranging from 3- to 16-fold higher than in the MABA. A single thioether derivative (**4j**) within the Rif S series shows a unique profile with modest, albeit essentially equivalent, potency in both MABA and LORA (2.0 vs 1.3 μM, respectively). Amine adducts within the RMP S (**8a**–**8f**) and RMP (**10a**–**10f**) series display similar potencies as the Rif S series in the MABA (MIC_{90}s 3.6–4.7 μM) and the LORA (MIC_{90}s 13.7–19.2 μM), with a 3.5- to 5-fold differential between the two assays. Core-modified pyrazole analogues within both Rif S (**5**) and RMP S (**9a**, **9b**) series are weakly to moderately active with MIC_{90}s of 3.9–5.4 μM in the MABA and >18.6 μM in the LORA. Surprising and especially noteworthy are the potencies of the tosylated intermediates. Rif S tosylate (**3**) shows MIC_{90}s of 0.20 μM in the MABA and 3.0 μM in the LORA, and RMP S tosylate (**7**) 0.24 μM and 4.8 μM, respectively, in the two assays. To determine if this was due to a prodrug effect from simple sulfonate hydrolysis to parent compounds **2** and **6**, respectively, we subjected each tosylate to conditions utilized for MIC determinations (buffer, 37 °C, 24 h) and the RNAP assay (*vide infra*; buffer, 37 °C, 2 h). At the end of the assay period, the medium was extracted with ethyl acetate and the organic extract was analyzed by thin-layer chromatography for the presence of either parent phenol or corresponding tosylate. In all cases, only the presence of tosylate was observed. In summary, none of the amine or pyrazole derivatives show superior microbiological properties to their parent scaffolds in the MABA and LORA. The tosylated (**3** and **7**) and thioether (**4j**) derivatives display surprising low MIC_{90}s, which are corroborated by excellent potency toward the target RNAP enzyme (*vide infra*).

As reported earlier, the activity and inhibition (by commercially available rifamycins) of wild-type (WT) and rifamycin-resistant MTB RNAPs has been assessed via an in vitro rolling circle transcription assay.[21] Twelve β subunit residues interact with rifampin where the S450 residue is involved in directly forming a hydrogen bond with the C-8 hydroxyl group. To determine the IC_{50} values (the concentration that results in 50% inhibition of transcription) of these analogues, the mutant MTB RNAP (S450L) was assessed along with the WT MTB RNAP (Table 2, S-Table 1, S-Fig. 1). For the WT MTB RNAP, RMP (**1**), Rif S (**2**), thioether **4j** and RMP S (**6**) show the highest activities with IC_{50} values in the low nM range. The IC_{50} values for RMP (**1**) and Rif S (**2**) were determined to be less than 10 nM. However, the amount of enzyme used in each reaction was 10 nM (the lowest concentration that we could confidently use). Under these conditions, it is possible that a 10 nM IC_{50} may simply reflect the 'titration' of the enzyme by an inhibitor with a much lower true IC_{50}. We have therefore elected to report any IC_{50} determined to be less than 10 nM as simply '<0.01' μM.

As mentioned above, the tosylated intermediates **3** & **7** have comparable MTB MIC_{90} values for both MABA and LORA; however, the IC_{50} value with WT MTB RNAP for **7** is ~seven-fold greater than that for **3**. The IC_{50} value of **3** (21 nM) is ~two-fold greater than the IC_{50} value of Rif S (<10 nM) with the WT MTB RNAP. Owing to the fact that the MABA MIC_{90} value for **3** is five-fold greater than that for Rif S, a parallel decrease in potency is observed for both the MIC_{90} and IC_{50} values for **3** in comparison with Rif S. However for compound **7**, this trend is not as quantitative. The IC_{50} value with WT MTB RNAP for **7** (142 nM) is more than 10-fold greater than the IC_{50} value for RMP S (13 nM); whereas, the MABA MIC_{90} value of **7** is only ~three-fold greater than that for RMP S. Surprisingly for the MTB RNAP (S450L) mutant, a lower IC_{50} value is observed for **7** (~nine-fold lower) than the IC_{50} value of **3**. Within the Rif S series, the amino analogues (**4a**, **4c**, and **4i**) that had exhibited modest MIC_{90} values under aerobic conditions have much more variable IC_{50} values (~70- to 2000-fold greater than Rif S). These analogues have comparable IC_{50} values against the MTB RNAP (S450L) mutant, which are still 3- to 8-fold greater than Rif S. The thioether derivative (**4j**) also exhibits modest MABA MIC_{90} values, but the IC_{50} values are comparable to the IC_{50} values

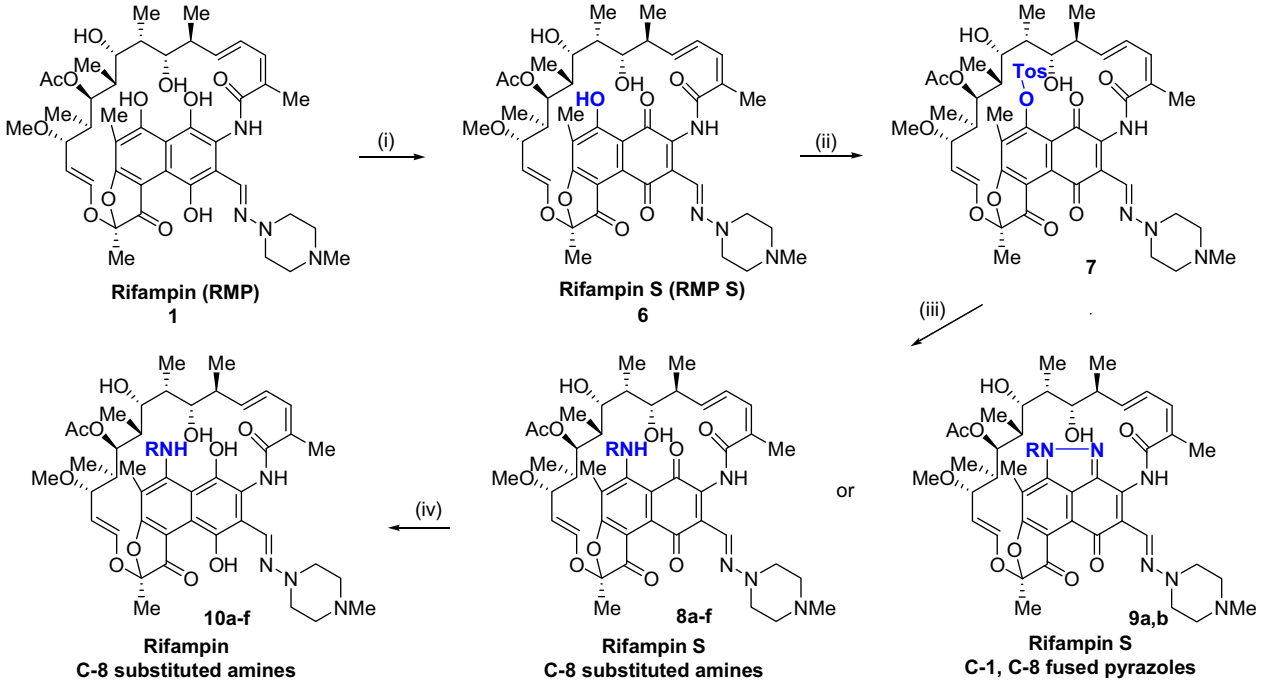

Scheme 2. Synthesis of C-8 analogues of rifampin and rifampin S. (i) potassium ferricyanide, pH 7.4 phosphate buffer, ethyl acetate; (ii) *p* toluenesulfonyl chloride, diisopropylethylamine, acetonitrile; (iii) RNH_2, or $RNHNH_2$ in acetonitrile (33–60% yield); (iv) ascorbic acid, methanol (51–93% yield).

Table 1
Screening results of rifamycin analogues versus MTB

No.	Class	C-8 Substituent	MTB MIC_{90} (μM)[a]	
			MABA	LORA
2	Rif S	Hydroxyl	0.03	0.4
3	Rif S	Tosyloxy	0.20	3.0
4a	Rif S	Amino	1.41	22.2
4b	Rif S	Methylamino	>5.6	20.6
4c	Rif S	Dimethylamino	1.8	5.4
4d	Rif S	Ethylamino	5.5	21.4
4e	Rif S	Methoxyamino	3.8	12.5
4f	Rif S	*N*-(2-propenyl)amino	5.2	18.3
4g	Rif S	(2-Hydroxyethyl)amino	5.32	>21.7
4h	Rif S	Benzylamino	2.4	>20.4
4i	Rif S	Cycloheptylamino	2.2	>20.2
4j	Rif S	Methylthio	2.0	1.3
5	Rif S pyrazole	2-Hydroxyethyl	>5.4	>21.7
6	RMP S	Hydroxyl	0.07	0.5
7	RMP S	Tosyloxy	0.24	4.8
8a	RMP S	Methylamino	3.64	>19.2
8b	RMP S	Ethylamino	>4.7	>18.9
8c	RMP S	*N*-(2-propenyl)amino	>4.7	>18.6
8e	RMP S	(2-Hydroxyethyl)amino	>4.6	>18.5
8f	RMP S	Benzylamino	>4.4	>17.6
8g	RMP S	Cycloheptylamino	3.9	13.7
9a	RMP S pyrazole	Methyl	>4.8	>19.3
9b	RMP S pyrazole	2-Hydroxyethyl	3.9	>18.6
10a	RMP	Methylamino	4.0	>19.1
10b	RMP	Ethylamino	>4.7	>18.8
10c	RMP	*N*-(2-propenyl)amino	>4.6	>18.6
10d	RMP	(2-Hydroxyethyl)amino	>4.6	>18.5
10e	RMP	Benzylamino	>4.4	>17.5
10f	RMP	Cycloheptylamino	3.8	>17.4
1 (RMP)		Hydroxyl	0.13	1.9
Isoniazid		N/A[b]	0.39	>128
PA824		N/A	0.66	2.3
Moxifloxacin		N/A	0.64	4.3

[a] The MIC_{90} is defined as the minimum concentration of the compound required to inhibit 90% of bacterial growth.
[b] N/A = not applicable.

Table 2
Selected rifamycins versus MTB RNAP and *E. coli*

No.	IC_{50} (μM)[a] (WT MTB RNAP)	IC_{50} (μM)[a] (MTB RNAP (S450L))	*E. coli* MIC_{90} (μM)[b]		
			TG2	DH5α	EC28880
1	<0.01	52.1	12.5	12.5	0.1
2	<0.01	36.0	100	>100	0.78
3	0.021	982	>100	>100	3.125
4a	4.4	186	>100	>100	12.5
4c	0.503	270	>100	>100	12.5
4i	15.4	127	>100	>100	>12.5
4j	0.015	37.5	>100	>100	>12.5
6	0.013	46.5	12.5	25	0.1
7	0.142	111	>100	>100	12.5
9b	0.139	29.9	>100	>100	>12.5

[a] The IC_{50} is defined as the concentration that results in 50% inhibition of transcription. (The experimental conditions are reported in the Supplementary data).
[b] See footnote a, Table 1. (The experimental conditions are reported in the Supplementary data).

observed for the controls (**1, 2, 6**) with both WT MTB RNAP and the mutant. Although the pyrazole analogue (**9b**) is weakly active microbiologically with higher MTB MIC_{90} values, the IC_{50} value is comparable to that observed for **7** (both about 10- to 20-fold higher than those for RMP, RMP S and Rif S). All rifamycin analogues have MTB MIC_{90} values that are higher than their IC_{50} values for the MTB RNAP with the exception of **4i**. This differential between IC_{50} and MTB MIC_{90} may be due in some cases (where the differential is large) to the molecules not equilibrating efficiently across the cell envelop or to the more trivial explanation (in cases where the differential is small) that the IC_{50} is a 50% inhibition point whereas the MIC_{90} is a 90% inhibition point. In the case of **4i**, the analogue has an MTB MIC_{90} that is approximately eight-fold smaller than the IC_{50}. One possibility is that the cycloheptyl moiety of **4i** may help to concentrate the analogue within the MTB cell. No analogues tested here result in a more potent rifamycin derivative against the MTB RNAP (S450L) mutant.

The IC_{50} values have also been previously determined for the *Escherichia coli* RNAP.[21] It was observed that both MTB and *E. coli* enzymes exhibited similar trends, with IC_{50} values in the 10^{-9} M (nM) range for commercially available rifamycins tested. This observation is consistent with previous postulates that the lower sensitivity of Gram-negative bacteria to rifamycins is due to the removal of rifamycins from the interior of the cell via TolC-dependent efflux pumps. To probe that same efflux activity with our novel analogues, we have determined the MIC_{90} values of a subset of our compounds using WT *E. coli* strains (TG2 and DH5α) and a mutant *E. coli* strain (EC2880-'permeable' strain, *tolC*$^-$ and *imp*$^-$). Generally, the mutant *E. coli* strain is more sensitive than the WT strains to tested rifamycins. Interestingly, the MIC_{90} value for compound **3** is only four-fold greater than that observed for Rif S. This parallels compound **3**'s IC_{50} value, which is 3–4 higher than that for Rif S. The results in Table 2 indicate that the rifamycins tested are subject to Gram-negative efflux pump activity.

To gain better understanding of the SAR, we carried out structure-based modeling studies. Modeling was based on the 2.5 Å resolution structure of rifabutin complexed with the *Thermus thermophilus* RNAP holoenzyme (PDB ID: 2a68).[22] Since the rifamycin binding site is highly conserved among bacteria, this structure provides a good foundation for understanding how proposed rifamycin analogues may interact with the MTB RNA polymerase. Preparation of the structure before modeling is described in the Supplementary data and was conducted using MOE.[23]

Given the size of the rifamycins, size of the binding site, and the flexibility of the ansa ring, accurate docking of these inhibitors to the RNAP complex would be challenging using standard docking approaches. Since most of the rifamycin structure remains unchanged, modeled poses of the analogues were generated by mutating rifamycin to the analogue and then relaxing the complex through a series of energy minimizations as described in the Supplementary data.

Modeled poses were generated for each of the structures listed in Table 2. A QSAR model (not shown) using interaction energies between the inhibitor and RNAP complex and two other ligand descriptors produced a very good R^2 of 0.90 and a cross validation R^2 of 0.79. The good fit of the QSAR model based on energies from the structure-based modeling supports the accuracy of the latter. The robustness of our structure-based modeling has also been supported by experimental studies where sensitivity to rifamycins against binding site mutants qualitatively correlates with our models.[21] The QSAR model will be presented elsewhere.

Modeled poses for Rif S (**2**) and amino analogue (**4i**) are shown in Figure 1. RNAP is shown as a molecular surface within 5 Å of the inhibitors and shaded to indicate areas of lipophilicity (green), hydrogen bonding (magenta) and mild polar (blue). This figure illustrates how the loss of the C-8 hydroxyl is a potential loss of a hydrogen bond contact with RNAP.

One of the clinical liabilities of RMP (**1**) includes its induction of cytochrome P450 3A4 (CYP3A4), which is mediated by the Human Pregnane X Receptor (PXR).[12] Therefore we utilized a commercially available assay kit[24] to examine if representative analogues (**8a**, **9a**, and **10a**) activate the PXR. The results (Table 3, Fig. 2, S-Fig. 2) show that the methylamino derivatives of RMP S (**8a**) and RMP (**10a**) do activate the PXR to an extent very similar to that for rifampin, whereas the RMP S pyrazole derivative (**9a**) does not exhibit significant hPXR activation at concentrations up to 100 μM. From these data, we cannot yet address whether these analogues are Cyp inhibitors or substrates.

In summary, we have synthesized a novel series of rifamycin S and rifampin analogues incorporating substituted 8-amino, 8-thio, and 1,8-pyrazole substituents. Screening the compounds for inhibition of WT *M. tuberculosis* (MTB) RNAP and rifamycin-resistant MTB RNAP (S450L) as well as antitubercular effects under both aerobic and anaerobic conditions show that our modification of the 8-OH position of the parent scaffolds results in diminished activity. The enzymatic and microbiological data are consistent with modeling and computational studies which support the C-8 hydroxyl acting as a hydrogen bond acceptor with S450 and that Rif resistance in the S450L mutant is due to loss of this hydrogen bond. Data on representative analogues of this study suggest that only the pyrazole modification to the rifamycin parent scaffold minimizes hPXR activation.

Table 3
PXR activity of selected rifamycin analogues

No.	EC_{50} (μM)[a]	E_{MAX}[b] (fold increase)
1	5.6	9.5
8a	2.1	6.9
9a	nda[c]	nda
10a	4.1	8.9

[a] EC_{50} is defined as the half maximal effective concentration.
[b] EC_{MAX} is the maximal effective concentration of the compound. (The experimental conditions are reported in the Supplementary data).
[c] nda: no detectable activation of hPXR at concentrations up to 100 μM.

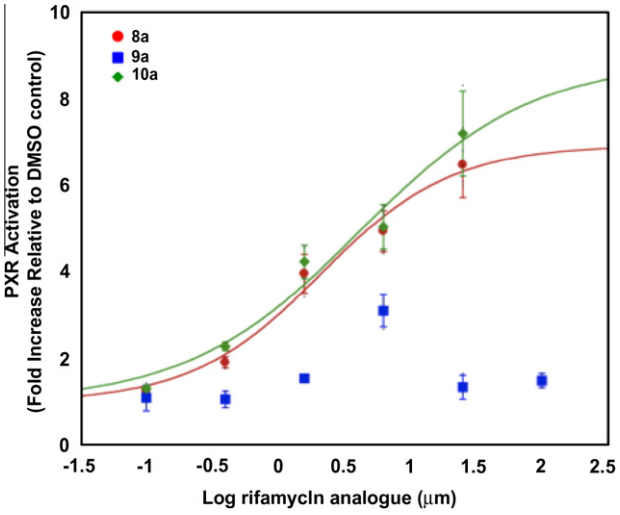

Figure 2. Selected rifamycin analogues versus PXR activation.

Acknowledgments

We acknowledge generous support by the University of Michigan College of Pharmacy Ella and Hans Vahlteich and UpJohn Research Funds. We would also like to acknowledge additional funding by the University of Michigan Office of the Vice President for Research, and the Rackham Graduate School.

Supplementary data

Supplementary data (details of the chemical syntheses, the in vitro RNAP assays, molecular modeling, and the human pregnane X receptor (PXR) activation assay) associated with this article can be found, in the online version, at doi:10.1016/j.bmcl.2011.08.054.

References and notes

1. WHO. WHO Report 2008.
2. Mitchison, D. A. *Front. Biosci.* **2004**, *9*, 1059.
3. Schmidt, M. W.; Baldridge, K. K.; Boatz, J. A.; Elbert, S. T.; Gordon, M. S.; Jensen, J. H.; Koseki, S.; Matsunaga, N.; Nguyen, K. A.; Su, S. J.; Windus, T. L.; Dupuis, M.; Montgomery, J. A. *J. Comput. Chem.* **1993**, *14*, 1347.
4. Calvori, C.; Frontali, L.; Leoni, L.; Tecce, G. *Nature* **1965**, *207*, 417.

5. Floss, H. G.; Yu, T.-W. *Chem. Rev.* **2005**, *105*, 621.
6. Hartmann, G.; Honikel, K. O.; Knusel, F.; Nuesch, J. *Biochim. Biophys. Acta* **1967**, *145*, 843.
7. Wehrli, W.; Nuesch, J.; Knusel, F.; Staehelin, M. *Biochim. Biophys. Acta* **1968**, *157*, 215.
8. Wehrli, W.; Staehelin, M. *Bacteriol. Rev.* **1971**, *35*, 290.
9. Wilhelm, J. M.; Oleinick, N. L.; Corcoran, J. W. *Biochim. Biophys. Acta* **1968**, *166*, 268.
10. McClure, W. R.; Cech, C. L. *J. Biol. Chem.* **1978**, *253*, 8949.
11. Campbell, E. A.; Korzheva, N.; Mustaev, A.; Murakami, K.; Nair, S.; Goldfarb, A.; Darst, S. A. *Cell* **2001**, *104*, 901.
12. Aristoff, P. A.; Garcia, G. A.; Kirchhoff, P. D.; Showalter, H. D. H. *Tuberculosis* **2010**, *90*, 94.
13. Wehrli, W.; Staehelin, M. *Biochim. Biophys. Acta* **1969**, *182*, 24.
14. Dampier, M. F.; Chen, C.-W.; Whitlock, H. W., Jr. *J. Am. Chem. Soc.* **1976**, *98*, 7064.
15. Dampier, M. F.; Whitlock, H. W., Jr. *J. Am. Chem. Soc.* **1975**, *97*, 6254.
16. Showalter, H. D. H.; Berman, E. M.; Johnson, J. L.; Atwood, J. L.; Hunter, W. E. *Tetrahedron Lett.* **1985**, *26*, 157.
17. Marchi, E.; Montecchi, L. U.S. Patent 4,200,574, 1980.
18. Yamane, T.; Hashizume, T.; Yamashita, K.; Konishi, E.; Hosoe, K.; Hidaka, T.; Watanabe, K.; Kawaharada, H.; Yamamoto, T.; Kuze, F. *Chem. Pharm. Bull. (Tokyo)* **1993**, *41*, 148.
19. Collins, L.; Franzblau, S. *Antimicrob. Agents Chemother.* **1997**, *41*, 1004.
20. Cho, S. H.; Warit, S.; Wan, B.; Hwang, C. H.; Pauli, G. F.; Franzblau, S. G. *Antimicrob. Agents Chemother.* **2007**, *51*, 1380.
21. Gill, S. K.; Garcia, G. A. *Tuberculosis*, in press, doi:10.1016/j.tube.2011.05.002.
22. Artsimovitch, I.; Vassylyeva, M. N.; Svetlov, D.; Svetlov, V.; Perederina, A.; Igarashi, N.; Matsugaki, N.; Wakatsuki, S.; Tahirov, T. H.; Vassylyev, D. G. *Cell* **2005**, *122*, 351.
23. Molecular Operating Environment (MOE). Chemical Computing Group, Inc.: Montreal, 2010.
24. Human Pregnane X Receptor Activation Assay Kit; Puracyp, Inc.